

STUDIES OF SLIDING DISCHARGE IN GAS AT ATMOSPHERIC PRESSURE

G.P.Berezina, A.M.Yegorov, V.I.Karas', V.S.Us

National Scientific Center "Kharkov Institute of Physics & Technology", Kharkov, Ukraine,

karas@kipt.kharkov.ua

The aim of the study is to develop physical principles and methods of calculating efficient plasma-chemical reactors based on a sliding discharge at atmospheric pressure with pumping a gas mixture to decompose harmful compounds and to synthesize the compounds of use, and also to develop various ecologically clean processes. The necessity of wide-scale theoretical and experimental investigations, into the atmospheric-pressure gas discharge stems from: i) the importance for solving ecological and technological problems and ii) its inadequate study, as opposed to the case of discharges with tens of torrs, because of the difficulties of using the existing diagnostic facilities and even the methods of measurements at these parameters.

Studies were made into gas-dynamic and electrodynamic characteristics of TSD-based plasma-chemical reactors at positive and negative polarities of supply voltage applied to the wire-like electrode and for different rates of air flow through the reactors at different pressures inside the plasma-chemical chamber. The studies were made to optimize the plasma-chemical reactor design and to investigate the influence of different polarities of supply voltage to the wire electrode on the performance of the devices under consideration.

The electrodynamic SD characteristics were taken by the standard technique using standard instrumentation. The radiation spectra of high-pressure TSD were studied with an aid of the diffraction spectrograph DFS-452, the spectrograph SP 51, the diffraction monochromator MDR-12U and the photomultiplier tube PMT-39A in the 200 to 600 nm range.

1.Introduction

A method for treating gaseous effluents has appeared, called treatment by plasma [1-4]

2.Experimental studies into physical properties of the SD

At a positive potential across the wire, the discharge is ignited as a result of molecule and gaseous atom ionization in the region of high field intensity ($E \geq 3$ MV/m) in the vicinity of the anode wire. The electrons arrive to the anode in 10^{-7} - 10^{-8} sec leaving behind them the positive charge, and this still more increases the electric field strength. In turn, this favors the formation of the ionization wave propagating from the anode into the depth of the discharge gap with the result that the voltage needed to maintain the continuous discharge decreases as opposed to the case of negative polarity at the wire. At the same time, however, favorable conditions arise for creating local high-charge density regions in the discharge volume, at distances rather close to the flat cathode. And this, in turn, facilitates the conditions for jumping the discharge gap by the current channel and for the sparkover between the electrodes.

2.1.Experimental studies into electrodynamic and gas-dynamic characteristics of the sliding spark discharge

To investigate the processes have proposed to use a new-type plasma discharge, i.e., the sliding discharge at atmospheric pressure of the working gas, where a nonequilibrium weakly-ionized plasma is created with the electron temperature T_e much higher than the ion

temperature T_i and the neutral gas temperature T_0 .

To achieve this aim, it was necessary to develop and manufacture the flow-type plasma reactor, where the sliding discharge is ignited between two divergent electrodes and is propagating along them in the gas flow at atmospheric pressure. The ignition voltage is determined by the minimum spacing between the electrodes at the beginning of the system.

In view of the requirements on optimum steady-state nonequilibrium discharges, namely:

- the electron plasma density should be high enough to ensure the vibrational excitation of molecules passing through the gas;
- the average energy of nonequilibrium electron distribution must be of the same order of magnitude as the vibrational energy of gas molecules, but lower than the ionization energy,

the following discharge parameters were chosen: voltage 10 to 20 kV, current 0.1 to 1 A, the gas flow rate may vary from several m/s to several tens of m/s.

A pair of extended electrodes is located in the reactor chamber, whose design provides for:

- making the most use of the space between the conductors;
- a safe high-voltage supply to the electrodes (appropriate adjustment of spacing between them);
- variability in the angle of inclination between the electrodes;
- transparency of the reactor side walls for performing spectrography studies of the discharge;
- pumping the system along the gas flow direction under conditions of sufficient air tightness of the system.

The above-given technical requirements were taken into consideration on designing the plasma reactor. The reactor is in appearance a transparent dielectric chamber of rectangular section, measuring 50x200x1200 mm.

The reactor walls are made from a common glass, ~ 8 mm thick, the extended ends of the walls enter deep (~ 6 mm) into the grooves of the upper and lower flanges. A sheet acrylic plastic, about 25 mm in thickness, was used to manufacture the flanges. All the system is reliably fixed between two stainless steel end flanges of rectangular section. The mobility of reactor walls and extended flanges is totally excluded.

The reactor chamber entrance is connected via a special flange with a gas flow supply system which includes a fan with a controllable gas feed rate and an adapter manufactured from a multilayer rubber.

The reactor chamber accommodates two electrodes. One of them is a duralumin or steel plate, ~ 30 mm wide and ~1.5 mm thick, and the other is a copper pipe, 5 to 6 mm in diameter, or a duralumin or steel wire, 0.5 to 1.5 mm in diameter. The lower electrode is fixed on the acrylic plastic flange. The upper electrode is mounted on the upper acrylic plastic flange in such a way that the distance of each of its end with respect to the lower electrode can be varied independently. This provides a possibility of setting the required angle between the electrodes at the beginning of the chamber. The electrodes are connected with the power source via the top and bottom flanges of the reactor.

The reactor also comprises a pair of additional electrodes located immediately before the extended electrodes. They are used to ignite a spark or arc discharge. Under the action of the gas flow the arc is drawn into the gap between the main discharge electrodes and this essentially facilitates the initial breakdown between them at appreciably greater interelectrode spacings. The additional electrodes are the two copper rods, being in opposition to each other, have molybdenum or tungsten rod extension pieces. When the wire is worn by sparking, the interelectrode spacing can be smoothly adjusted.

The two extended electrodes can be easily moved along the reactor axis within 15 to 20 cm, either approaching the arc discharge electrodes or receding from them.

The reactor has been made as a pilot model which can quickly be adapted to the required electrode configuration, to evaluation of different materials from which the electrodes are made, and also to introduction of diagnostic probes, probes for igniting the arc discharge associated with the synchronous diagnostics start system (to take oscillograms of the respective signals), etc.

The two sets of electrodes (extended and arc) are fed from two supply sources: 25 kV, 300 A and 15 kV, 500 A, respectively. The supply system of extended discharge electrodes includes a regulating two-phase transformer, a high-voltage transformer, a diode D1008-based Gratz rectifier, a Π -shaped filter with a choke and a $0.5\text{mf}\times 25\text{kV}$ (type KBG-P) capacitor, a KEV-20 \times 2 MO discharge resistor, a kilovoltmeter C-96. The arc-

electrode supply unit consists of a regulating transformer, a high-voltage three-phase transformer, a diode KT5201D-based Larionov rectifier and a kilovoltmeter C-196.

During operation a constant control over the discharge current and the voltage across the discharge gap was exercised. The voltage was controlled independently, i.e., across the source and directly across the electrodes (before R_b and after it). The discharge current is measured in the circuit between the low-voltage electrode and the ground (both the upper and lower electrodes can be grounded). The signal to the oscillograph comes in this case from a specially made inductance-free resistor. Under synchronous start-up conditions, the double-beam oscillograph S 8-14 with a memory took pictures of the current and the discharge voltage. The voltage was supplied from the corresponding attenuator. The processing of signals obtained made it possible to determine the $I-V$ discharge characteristics for various modes of operation which differed in the electrode shapes, materials of electrodes and their polarities.

A videocamera (Panasonic M-9000") was used to carry out visual observation and to study the sliding discharge velocity.

The discharge velocity was also determined using a set of probes located at regular intervals. The signals from each pair of probes went to the double-beam oscillograph. Given the interprobe distance and the delay time of one signal with respect to the other, the discharge motion velocity could be calculated.

The air volume pumped through the reactor was determined by measuring the dynamic resistance with an aid of the standard Venturi nozzle.

The discharge spectrum was investigated by means of a diffraction spectrograph DFS-452. The light from the discharge, that was taken from the open end of the P-C reactor on the mirror, was projected onto the spectrograph slit restricted in height by a diaphragm. The spectrum was taken in the operating range of spectrograph wavelengths from 190 to 1100 nm.

A 600 lines/mm first-order grating was used in the measurements. Considering that on using this grating the photofilm length can cover the spectrum part of no more than 330 nm, all the range was divided into parts, each being photographed on a separate film with different light filters, namely, BS-10 for operation in the spectrum range from 360 to 730 nm and the KS-19 for the 720-1100 nm range. These light filters were used to cut off other orders of the spectrum. For comparison purposes, reference spectrograms of hydrogen, mercury- and sodium-vapor lamps in the corresponding ranges were applied to the film.

The voltage of the supply source was kept constant, $U_0 = 17$ kV. At the beginning of measurements, the maximum interelectrode spacing was determined, at which the self-sustained discharge propagated in the air flow along the whole length of the electrodes. The interelectrode spacing was then increased by 0.2 to 0.3×10^{-2} m, and the discharge was ignited through the use of high-voltage pulses coming to the additional

electrode from the spark device.

The oscillographs with memory and the spark device

From fig.1 and fig.2 it is seen that at low discharge currents the comparison between the curves given in curves exhibit a clearly marked sloping part (negative-resistance part). At high discharge currents, the discharge gap resistance value becomes small and is weakly dependent on the current value. The discharge with these $I - V$ characteristics is intermediate in the discharge classification between the glow discharge and the arc discharge. It should be noted that the E/N value is rather low in the discharge under discussion at an arbitrary polarity of the voltage applied.

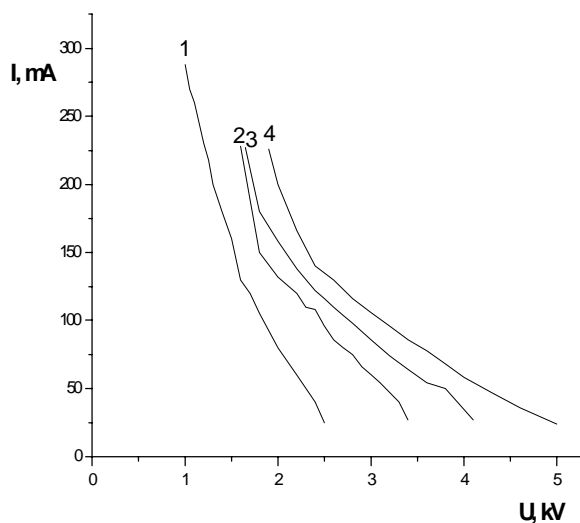


Fig. 1. $I - U$ curve of the sliding spark discharge with a negative potential at the wire electrode: 1 - $\tau = 10$ ms, 2 - $\tau = 30$ ms, 3 - $\tau = 50$ ms, 4 - $\tau = 70$ ms.

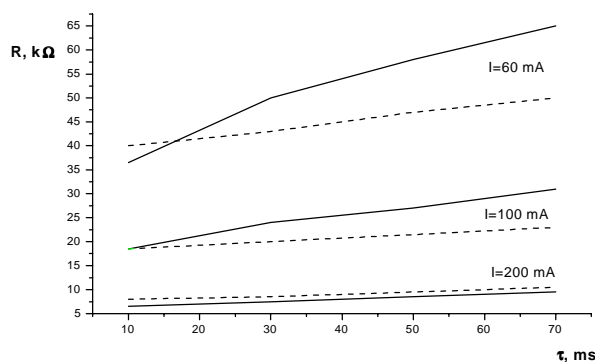


Fig. 2. Time dependence of the discharge resistance for different discharge currents and applied voltage polarities at positive (—) and negative (---) polarities of the wire electrode

It is seen from fig.2 that at low currents the time variation of resistance is much more prominent than at high currents. The increase in the discharge resistance with time is here connected with an increasing interelectrode distance as the discharge is propagating

were operated in the synchronous start mode. The start was controlled through the synchronizer. along the electrodes.

The velocity of discharge propagation along the electrodes was determined with an aid of a movable probe and through video shooting. In the first case, the probe was moved along the lower electrode. The probe received a portion of the discharge current at the instant Δt as the discharge traveled past it, this apparently depends on the distance between the discharge start and the probe, ΔL . Hence, the average discharge velocity at each part of the way ΔL can be readily calculated as $v = \Delta L / \Delta t$.

The velocities were measured at different discharge current values, different voltage polarities and discharge propagation lengths. In all the cases, the velocity was found to be the same, $v = 7.6$ m/s. It should be noted that the air pumping rate in the experiments was maintained to be the same.

As mentioned above, video shooting was also used to determine the velocity of discharge propagation. The shooting could be performed both in the usual (automatic) mode of operation and at fixed settings of the diaphragm, focus and exposure [from $(125 \text{ s})^{-1}$ to $(2000 \text{ s})^{-1}$] for a constant field frequency $f = 50$ Hz. The discharge was recorded on the film at three discharge current values with and without hooking up the capacitor to the discharge gap. Nearby the electrodes there is a scale marked every 5×10^{-2} m and 10^{-1} m. The videopictures were introduced to the computer.

Fig.3 shows the sequence of charge propagation for different conditions. It is seen from Fig.3 that the discharge propagates in $T = 2 \cdot 10^{-2}$ s over 0.15 m at the beginning and at the end of its path. So, the average velocity of discharge propagation is $v = 7.5$ m/s. Note that the discharge velocity depends neither on the discharge current nor on the polarity of voltage applied to the electrodes.

Thus, based on the two methods of measuring the velocity of discharge motion along the electrodes, it is found that, irrespective of the electrodynamic characteristics, the velocity of discharge motion is fully governed only by the gas flow characteristics. from the initial region (near the fan), to which either a pulsed voltage U_p from the modulator ($U_{p\text{max}} = 25$ kV, square pulse length is 1.5 ms) or the voltage from the power supply ($U_a = 8$ kV, current $I_a \sim 0.5$ A) was applied. In this case the voltage across the main electrodes was 1 or 2 kV lower than in the self-sustained discharge mode of operation. In the pulse mode, it was convenient, from the standpoint of better synchronization of oscillograph sweep with the onset of discharge, to operate at a repetition frequency of 1 Hz.

According to the above-given conclusions about the velocity of traveling spark discharge motion, it may be expected that with the fan of the rig that ensures a smooth adjustment of the flow velocity from 3 m/s to 10 m/s, the time of discharge propagation along the electrodes would be from 400 ms to 120ms, respectively.



Fig. 3. Sequence of charge propagation along the electrodes ($U_0 = 17$ kV)

- (a)- without a capacitor in the discharge gap, $R_b = 53$ k Ω , exposure time 1/500s;
 (b)- with a capacitor in the discharge gap, $R_b = 53$ k Ω , exposure time 1/500 s;
 (c)- without a capacitor in the discharge gap, $R_b = 53$ k Ω , exposure time 1/500 s;
 (d)- without a capacitor in the discharge gap, $R_b = 53$ k Ω , exposure time 1/500 s;
 (e)- with a capacitor in the discharge gap, $R_b = 53$ k Ω , exposure time 1/500 s;
 (f)- without a capacitor in the discharge gap, $R_b = 53$ k Ω , exposure time 1/50 s.

The reactor was used to perform the experiments with the spark discharge sliding due to the gas flow motion. The minimum interelectrode distance (at the start of discharge) varied within $(0.6$ to $1.6) \times 10^{-2}$ m; in this case, the independent spark discharge was struck at a voltage from 12 kV to 23 kV, depending on the shape, material and surface state of the electrodes. The rig also provides for the mode of operation corresponding to the semi-self-maintained discharge. For this purpose, two electrodes were accommodated at a distance of 3.0 cm

It is shown that the voltage from the modulator causes a spark discharge to occur between the additional electrodes with the result that intense high-frequency (10 to 20 MHz) oscillations are excited. In about 1 ms the traveling spark charge occurs between the main electrodes of the P-C reactor. In the circuit connected to the electrodes, intense HF oscillations are excited. Their frequency can be varied by means of external elements (e.g., a 4700 pF capacitor connected in parallel with the discharge). It is shown that oscillations occur at a frequency of 0.6 MHz, and in the absence of the capacitor their frequency was 2 MHz. The frequency of spark discharges occurring during discharge propagation

along the electrodes can be varied by the external elements and through the gas pumping speed.

Of special note is the influence of the transverse gas-flow component on the sliding discharge. It is shown that the transverse component leads to an increase in the dynamic resistance of the discharge, and thereby causes an increase in the specific electric field rather than a decrease in the current.

Preliminary spectrometry studies of the discharge were performed using the spectrograph ICP-51. Fig. 4 shows the radiation spectra of the discharge, where the cathode was a duralumin plate, and a steel wire, 1.5 mm in diameter, served as an anode; the interelectrode spacing linearly changes from 12 mm to 18 mm.

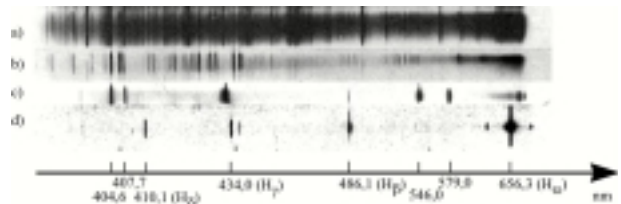


Fig. 4. Discharge radiation spectra ($U = 13.5$ kV, $I = 150$ mA): (a) - with an additional transverse air supply at an angle of 30° to the electrode axis; (b) - without an additional air supply; (c) - PRK-type mercury-quartz lamp radiation spectrum; (d) - hydrogen lamp radiation spectrum

The wavelength in all the spectrograms grows from left to right. Radiation spectra were also taken from the discharge, where the steel plate served as a cathode, and a steel wire, 1.5 mm in diameter, served as an anode, the other things remaining the same. The comparison between the spectra shows that for the range of traveling spark discharge parameters under study there are no spectral lines corresponding to the electrode materials, i.e., no sputtering of electrodes occurs in the discharge.

The treatment of the radiation spectra shows the presence of lines emitted by nitrogen molecules of the first $B^3\Pi \rightarrow A^3\Sigma$ and second $C^3\Pi \rightarrow B^3\Pi$ positive systems.

3. Conclusions

Wide-range theoretical and experimental investigations as well as computer simulation of the atmospheric-pressure sliding discharge have been performed with the use of present-day methods and techniques, and also a diverse diagnostic equipment.

- The findings for *the sliding spark discharge* are as follows:
- the velocity of the sliding spark discharge propagation is first measured using the probe system and video shooting; it is independent of the applied voltage polarity, of the electric current value and is coincident with the speed of air pumping along the discharge gap electrodes;
- high-frequency intense oscillations are excited in the discharge under study in two ranges, the frequency in the first range (tens of MHz) is independent of the parameters of external circuit elements, while the

frequency in the second range (hundreds of kHz up to 1 MHz) is specified by the circuit elements being external with respect to the discharge;

- using the transverse gas flow component can essentially change the dynamic resistance of the discharge, and thereby, the E/N value that determines the intensity of chemical reactions;
- in a wide current range, the radiation spectra of the discharge show do not show any spectral lines corresponding to the electrode materials.

The undertaken studies are an important stage in the comprehensive investigation of the atmospheric-pressure sliding discharge and they substantially add to the creation of physical principles and calculation methods of efficient plasma-chemical reactors, being of scientific and applied importance.

4. References

1. A.Czernichowski and H.Lesueur //Proceedings of NATO Advanced Research Workshop on Non Thermal Plasma Techniques for Pollution Control, Cambridge University, September 1992,p.61.
2. S.I. Krashennnikov, V.D.Rusanov, S.D.Sanyuk, and A.A.Fridman // Zh. Tekh. Fiz.,1986,v.56, p.1104. (in Russian).
- 3S.V,Saniuk, S.S.Kingsep, V.D.Rusanov, and A.Czernichovski //Proceedings of ISPC11, Loughborough UK, 1993, vol.2, p.740.
- 4 V,Dalaine, O.Martinie, J-M.Cormier, and P.Lefaucheux Destruction of H₂S by a sliding discharge with water //Proceedings of International Symposium on High Pressure, Low Temperature Plasma Chemistry. Cork, Ireland, August 1998, p.37.
5. . R.Pirs, A.Geidon. Otozhdestvlenie molekulyarnykh spektrov. M.: Inostrannaya Literatura, 1949. (in Russian).
6. N.Frank, S.Hirano, K.Kawamura // Radiat. Phys. Chem. 1988, vol.31, N1-3, p.57.
- 7 H.Hamba, O.Tokunaga, S.Sato, et al. // 3-rd Intern. Symposium “Global Environment and Nuclear Energy”, March 13, 1991, Japan.
8. B.M.Penetrante. NATO Advanced Research Workshop on Non-Thermal Plasma Techniques for Pollution Control (Cambridge University UK, September 21-25, 1992).
9. Yu.S.Akisev, A.A.Deryugin, V.B.Karal’nik, I.V. Kochetov, A.P.Napartovich, and N.I.Trushkin. Numerical Simulation and Experimental Study of an Atmosphere-Pressure Direct-Current Glow Discharge. Plasma Physics Reports. 1994. vol. 20, # 6, p. 511-524.
- 10 A.A. Valuyev, A.S. Kakliugin, et al. Radiation-plasmachemistry methods of smoke gas cleaning. Teplotekhnika Vysokikh Temperatur, 1990, vol. 28, # 5, p. 995-1008. (In Russian).
11. . Proc. VI Intern. Meeting of Radiation Processes. Ottawa, Canada, May-June, 1987; Rad. Phys. Chemistry, 1988, vol. 31, # 1-3.
12. . Jen-Shih Chang, P.A.Lawless, et.al. Corona Discharge Processes IEEE Trans. on Plasma Science, 1991, vol. 19. # 6, p. 1152-1165.
- 13.) Jen-Shih Chang. Advanced Corona Technology for Low Power Plasma Treatment of Combustion Flue Gases. Proceedings II-th International Symposium on High Pressure Low Temperature Plasma Chemistry. Poland, 1989, p. 103-108.
14. Yu.P.Raizer. Osnovy sovremennoy fiziki gazorazryadnykh protsessov. - M.: Nauka, 1980. (In Russian).
15. V.I.Karas’, V.V.Mukhin, A.M.Naboka, V.E.Novikov. On the electron and molecule kinetics in the beam- plasma discharge into molecular gases. Preprint KhIPhT # 87-18, 1987, p. 14. (In Russian)
- 16.G.P. Berezina. Collective Interaction of Nonrelativistic Electron Beam with Weakly-Ionized Plasma at High Gas Pressure. Doklady Akademii Nauk Ukrain-skoï SSR, Series A, 1989, # 7, p. 57-61.(In Russian).
- 17.L.A.Artsimovich. Thermonuclear reaction control. - Moscow: State Publishers of Physical and Mathematical Literature, 1961, p. 111-112. (In Russian).